Supporting Information

Preparation of antigen-responsive fluorogenic immunosensor by tyrosine chemical modification of antibody complementarity determining region

Shinichi Sato,*[a] Masaki Matsumura,[b, c] Hiroshi Ueda,[b] Hiroyuki Nakamura*[b]

(a) Frontier Research Institute for Interdisciplinary Sciences, Tohoku University, 2-1-1 Katahira, Aoba-ku, Sendai 980-8577, Japan
(b) Laboratory for Chemistry and Life Science, Institute of Innovative Research, Tokyo Institute of Technology, Yokohama, 226-8503, Japan
(c) School of Life Science and Engineering, Tokyo Institute of Technology, Yokohama, 226-8503, Japan

List of contents

1. Supporting Data

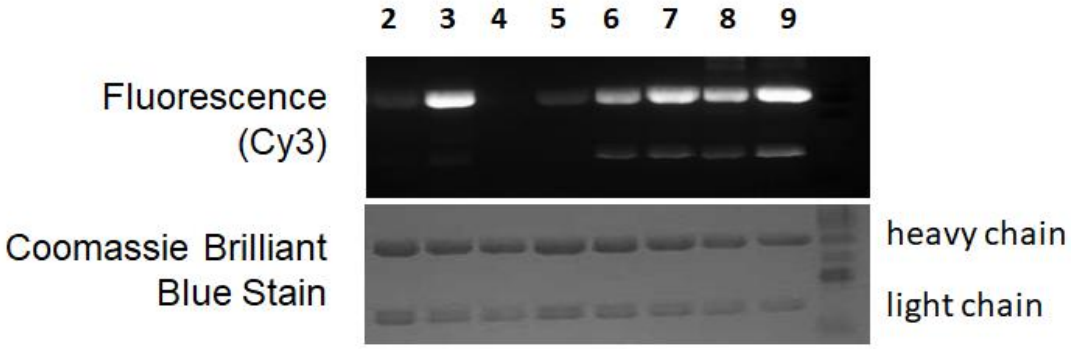

Figures S1. Comparison of rituximab modification efficiencies.

Reaction conditions: (step 1) rituximab (5 μM), horseradish peroxidase (HRP) (45 nM), H_2O_2 (25 μM), labeling reagent (300 μM) in tris buffered saline at room temperature for 1 h. (step 2) DBCO-Cy3 (25 μM) at 37 °C for 30 min.

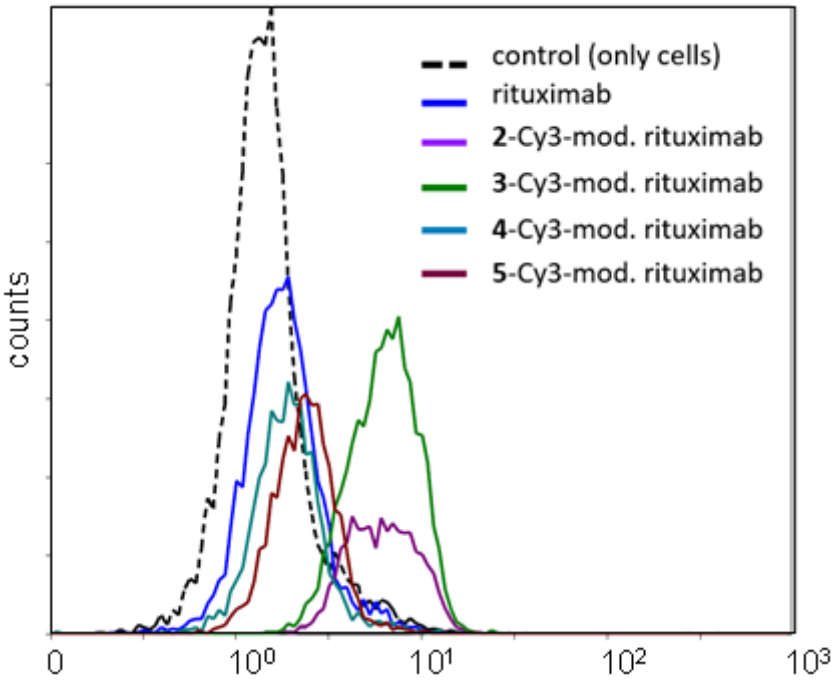

Figures S2. Fluorescence measurement on the SU-DHL-4 cells (CD20+) treated with Cy3-modified rituximabs. Modification reagents **2**–**5** were used at first step azide modification.

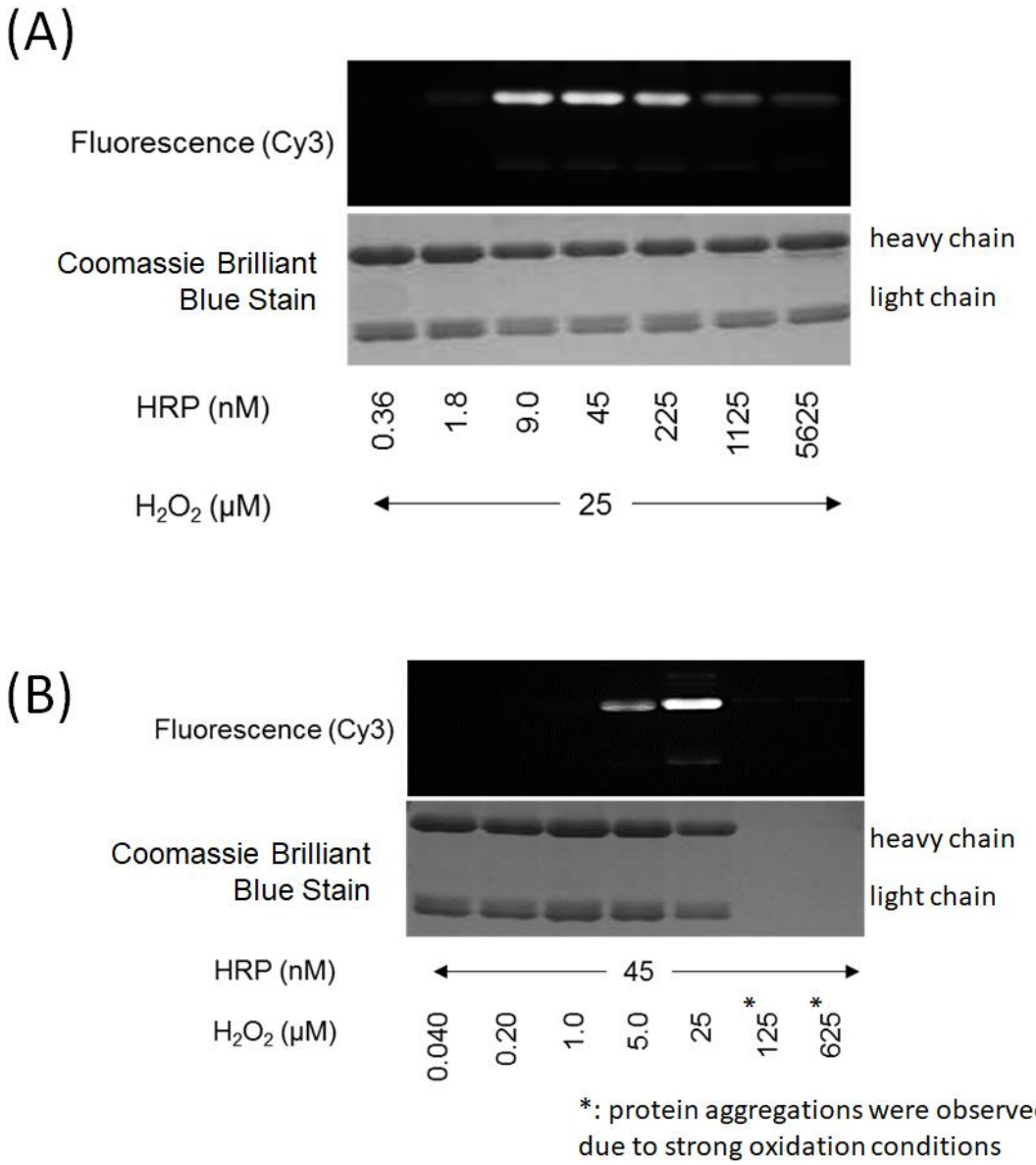

Figures S3. Optimization of rituximab modification condition. (A, B) Reaction conditions: (step 1) rituximab (5 μM), HRP (45 nM), H_2O_2 (0.36–5625 nM), labeling reagent (0.040–625 μM) in tris buffered saline at room temperature for 1 h. (step 2) DBCO-Cy3 (25 μM) at 37 °C for 30 min.

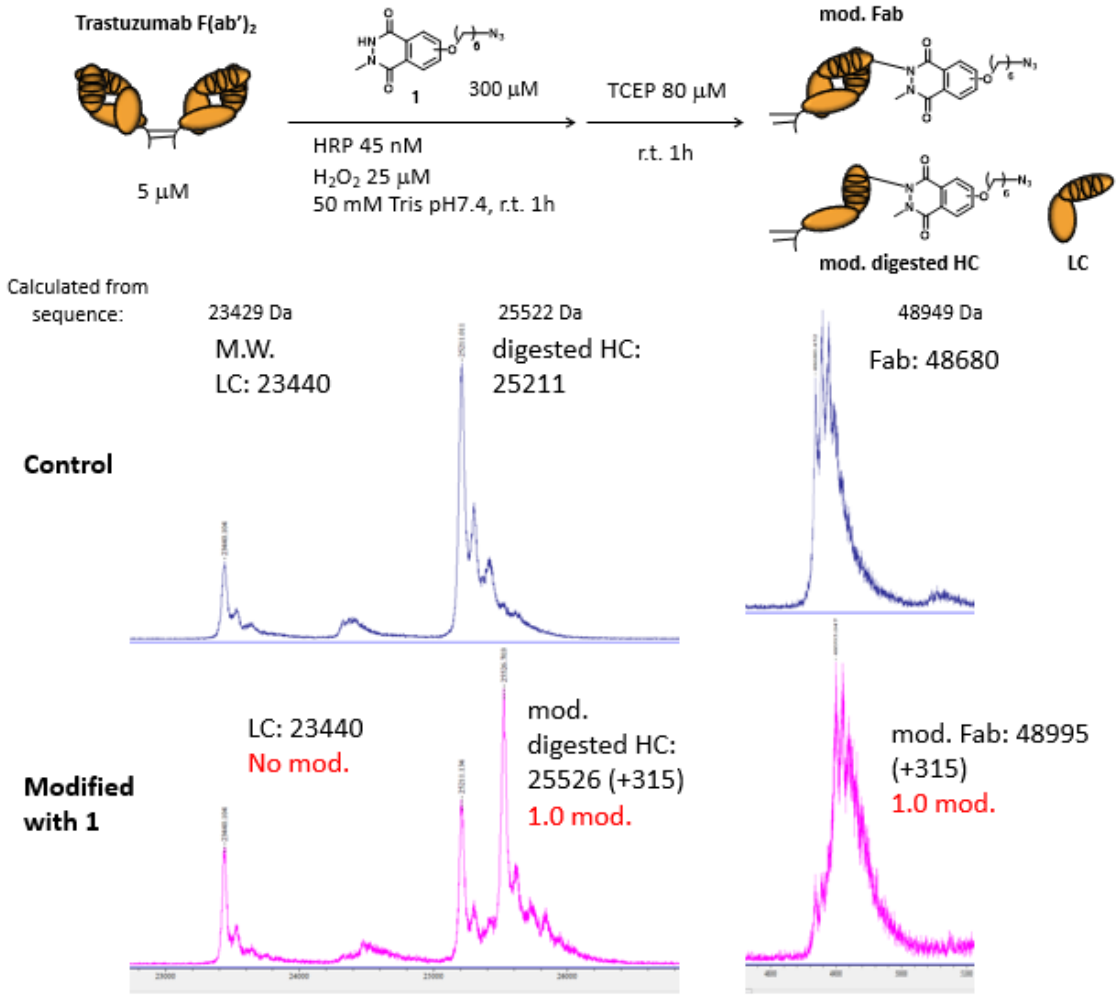

Figures S4. Intact mass analysis of trastuzumab modification.

In order to solve the difficulty of analyzing the MS peak of heavy chain due to the heterogeneity of glycoforms, we conducted an experiment using trastuzumab F(ab‘)$_2$. The trastuzumab F(ab’)$_2$ was found to be capable of selectively modifying heavy chains with the same efficiency as the full-length trastuzumab.[1] MS analysis under reducing conditions showed peak-shifts (monoadduct of 1) at the peaks corresponding to the heavy chain fragment and F (ab ‘), while the peak-shift was not observed at the peak corresponding to the light chain fragment

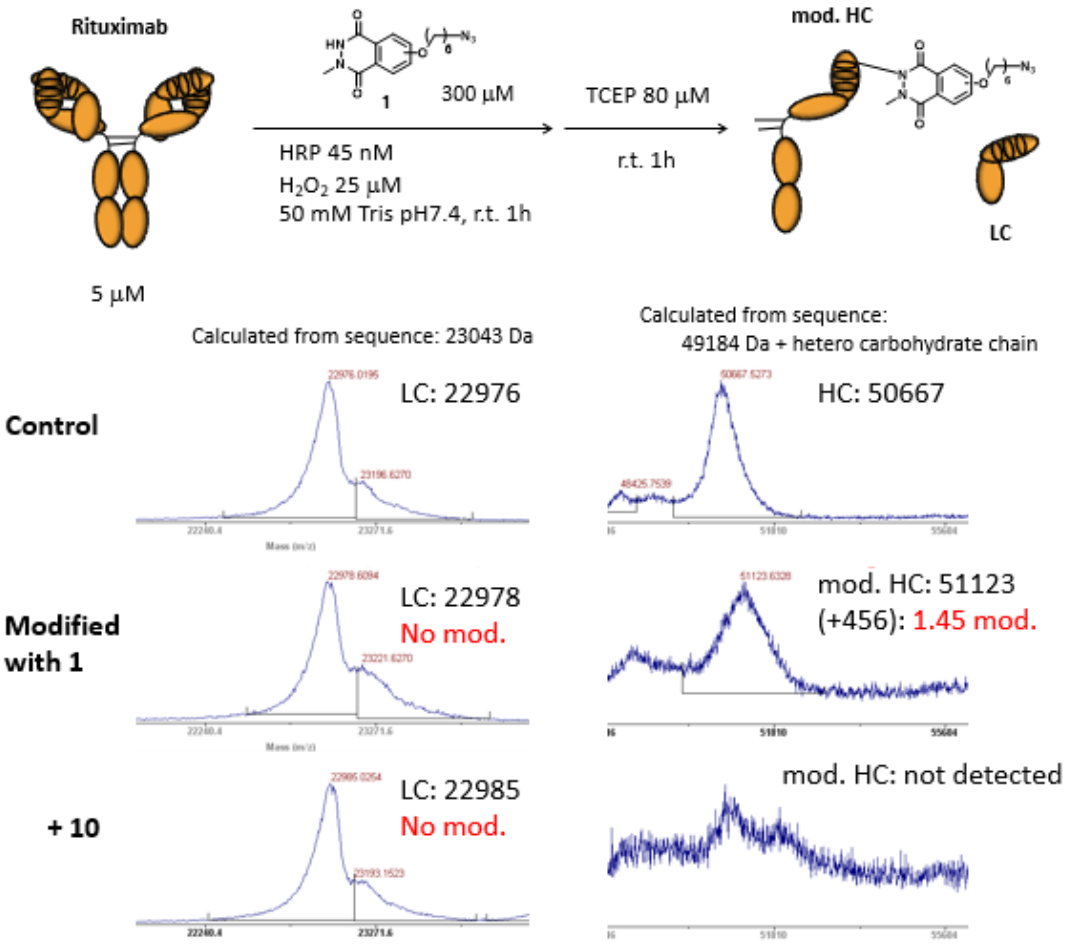

Figures S5. Intact mass analysis of rituximab modification.

Heavy chain-selective peak-shifts (average 1.45 molecules/ heavy chain) was observed, while the peak-shift was not observed at the peak corresponding to the light fragment.

For second step modification, modified peaks were not detected probably because it becomes less ionizable.

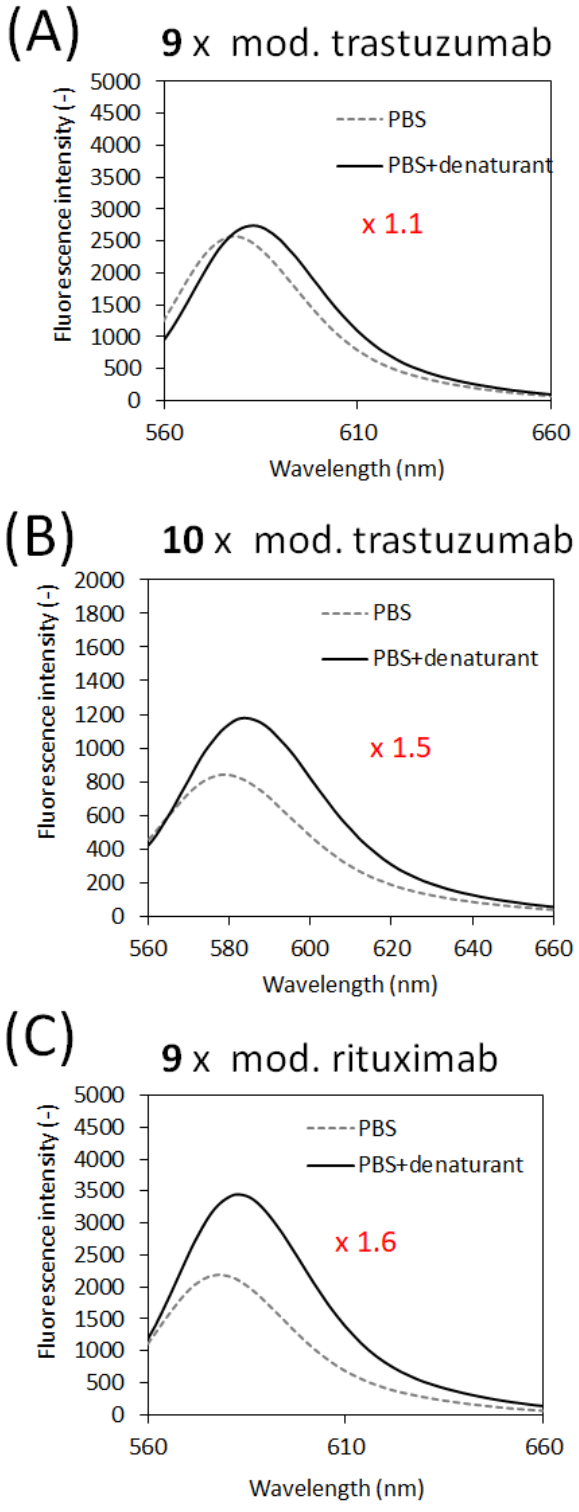

Figures S6. Fluorescent de-quenching by denaturation of antibodies modified in each condition. The antibody (trastuzumab or rituximab) modified with **1** in the first step was modified with **2** or **3** in the second step.

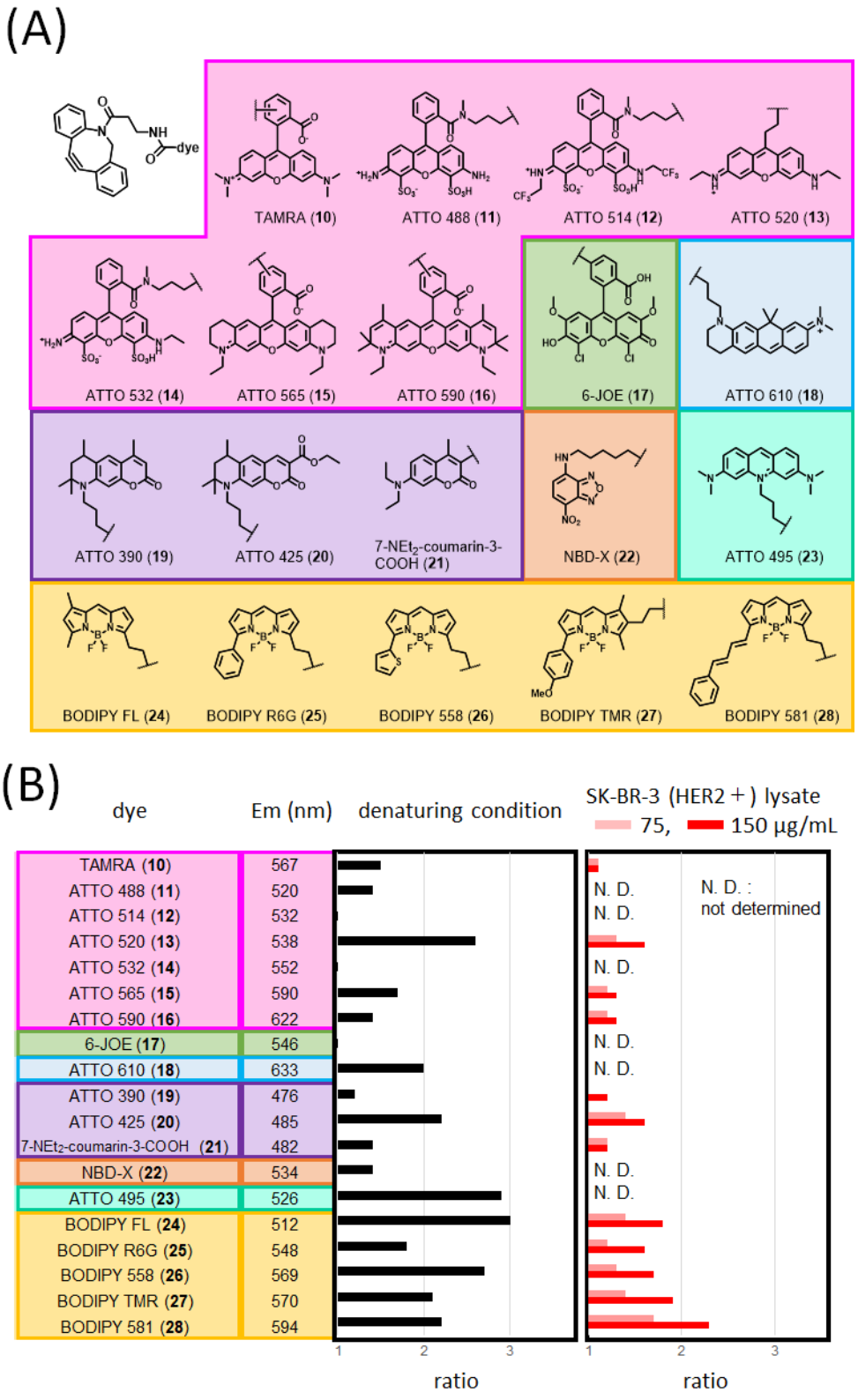

Figures S7. (A) Structures of tested fluorescent dyes. (B) Fluorescent response of modified trastuzumab.

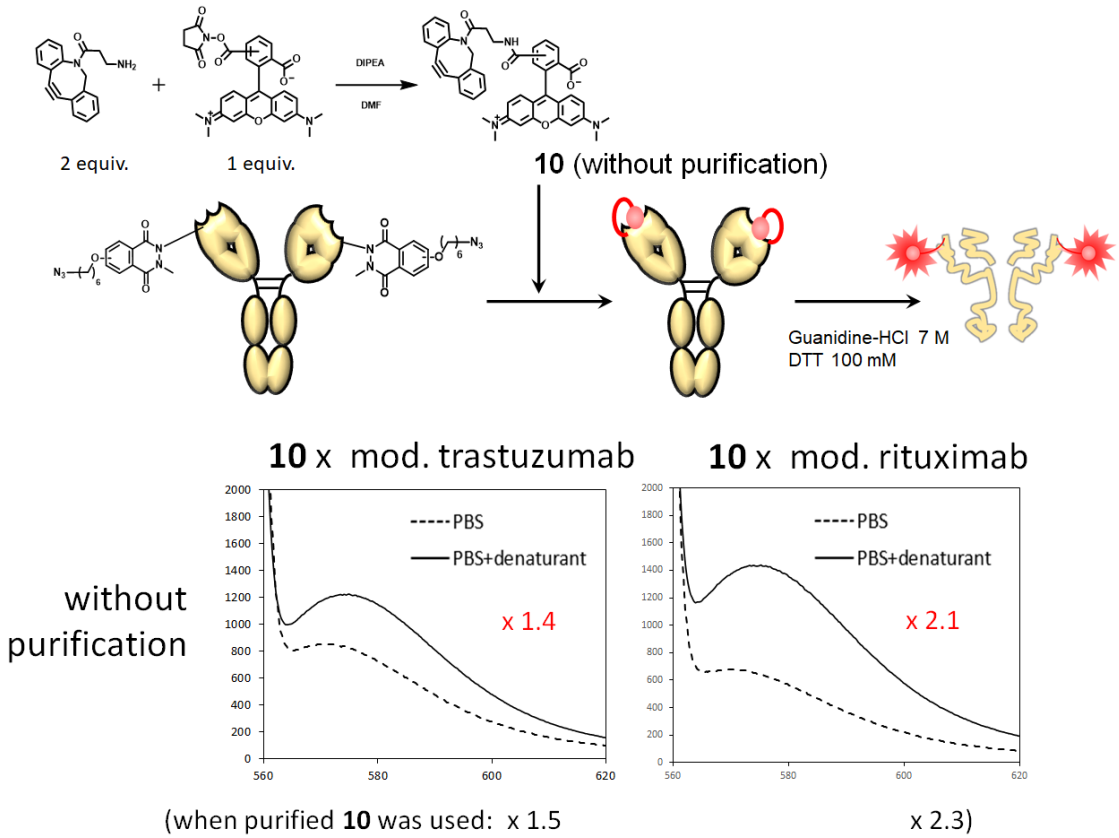

Figures S8. Comparison of fluorescent quenching effect between Q-bodies prepared by without-purification protocol and Q-bodies prepared with purified **10**.

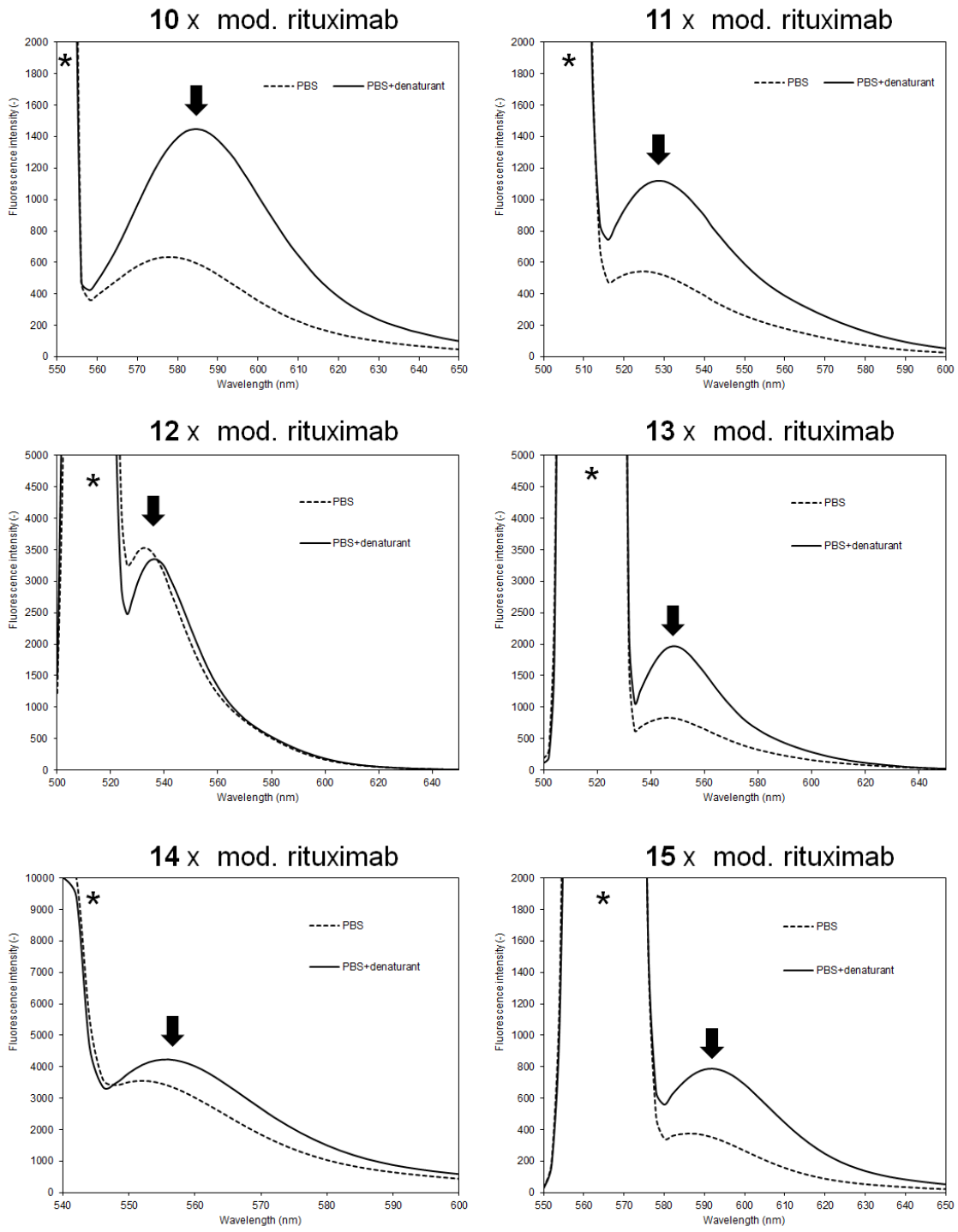

Figures S9. Fluorescent de-quenching of dye-modified rituximab in denaturing condition. Target emission signals are arrowed. *: Signal derived from the detection of excitation light.

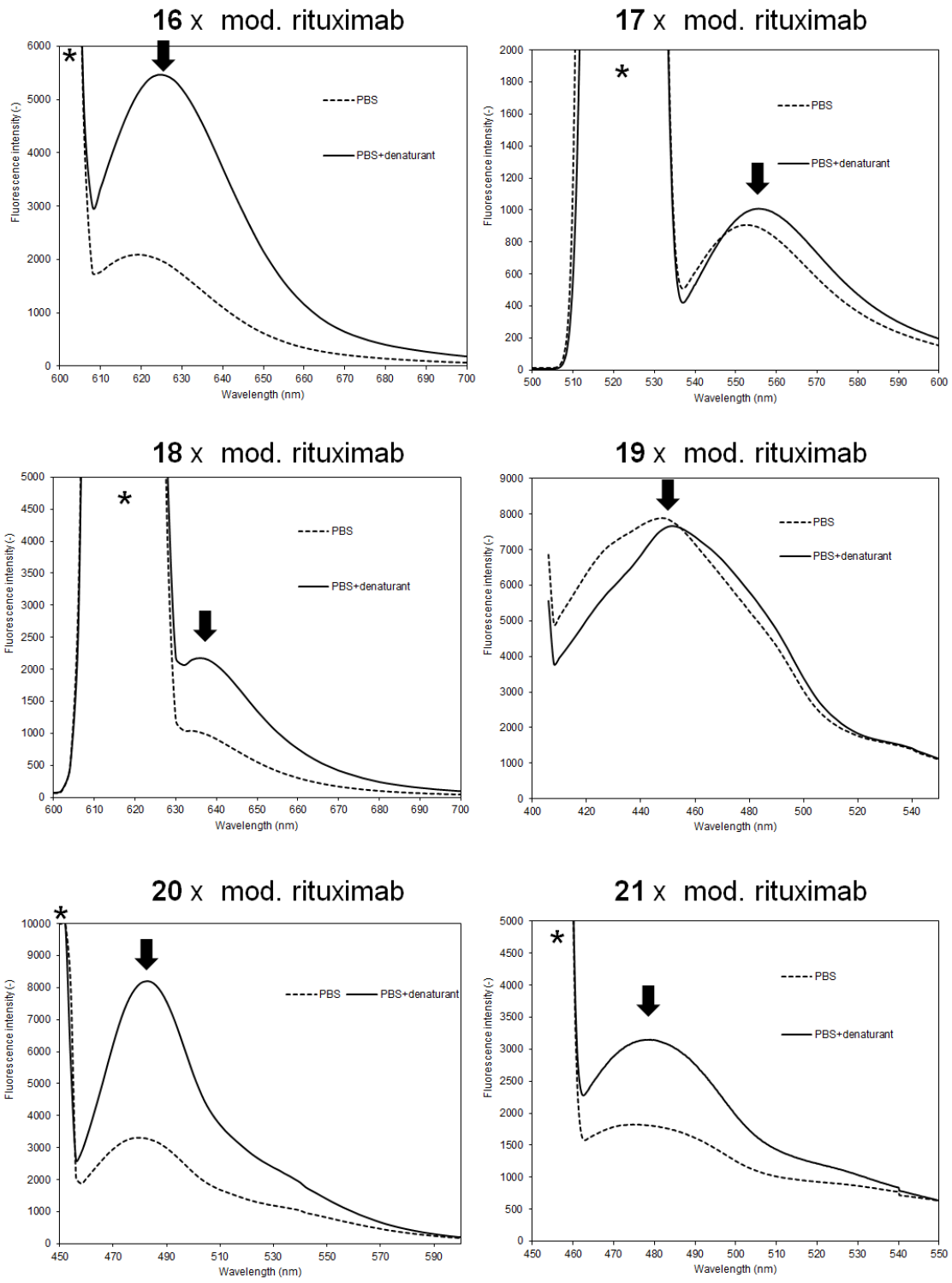

Figure S9 (continued).

Target emission signals are arrowed. *: Signal derived from the detection of excitation light.

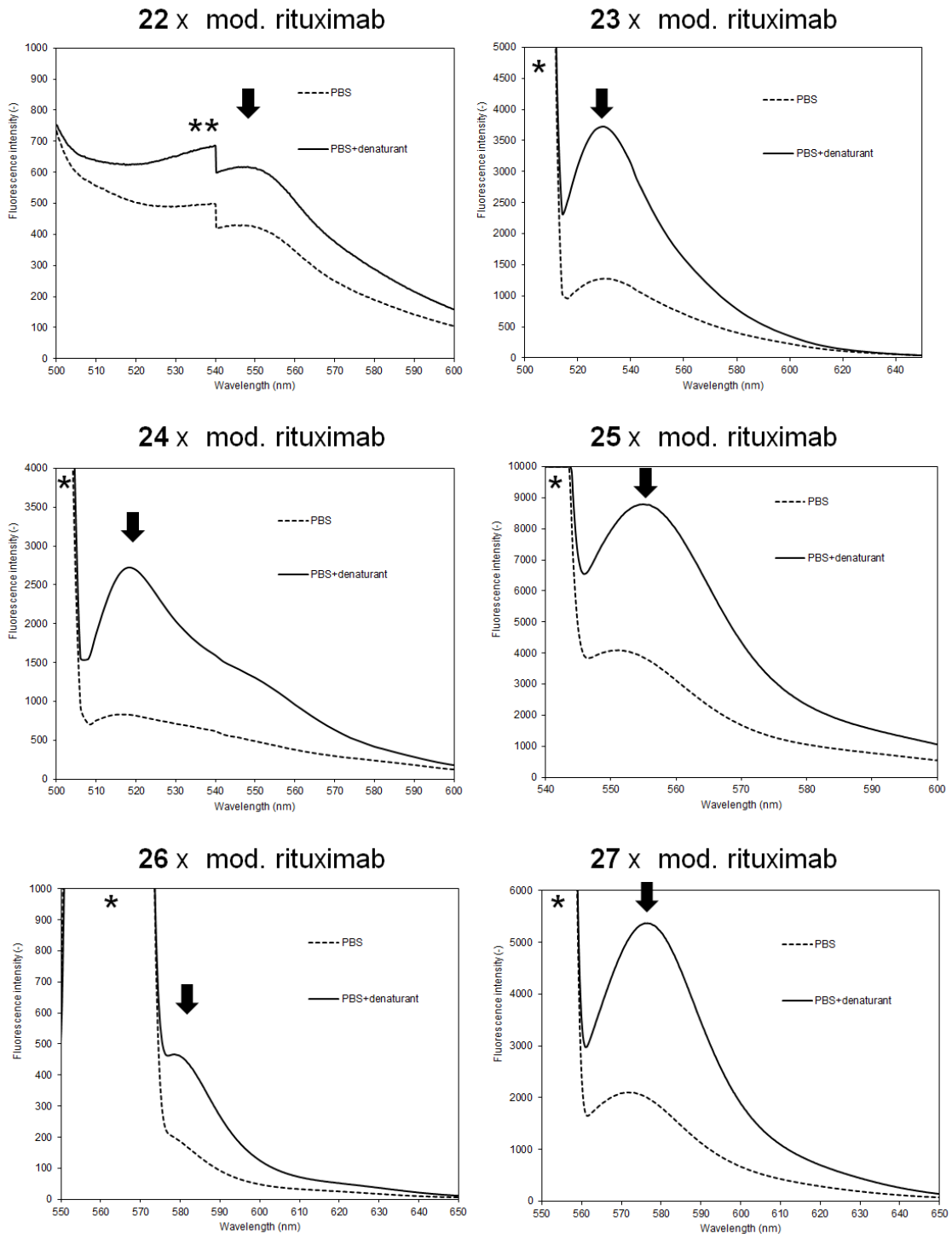

Figure S9 (continued).

Target emission signals are arrowed. *: Signal derived from the detection of excitation light.

**: Mechanical signal change for wavelength filter conversion

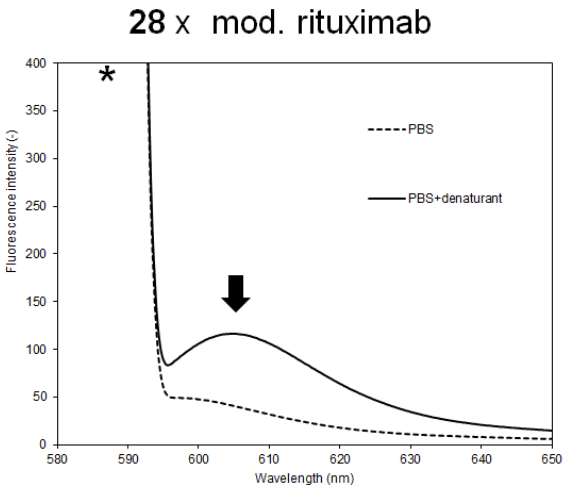

Figure S9 (continued).

Target emission signals are arrowed. *: Signal derived from the detection of excitation light.

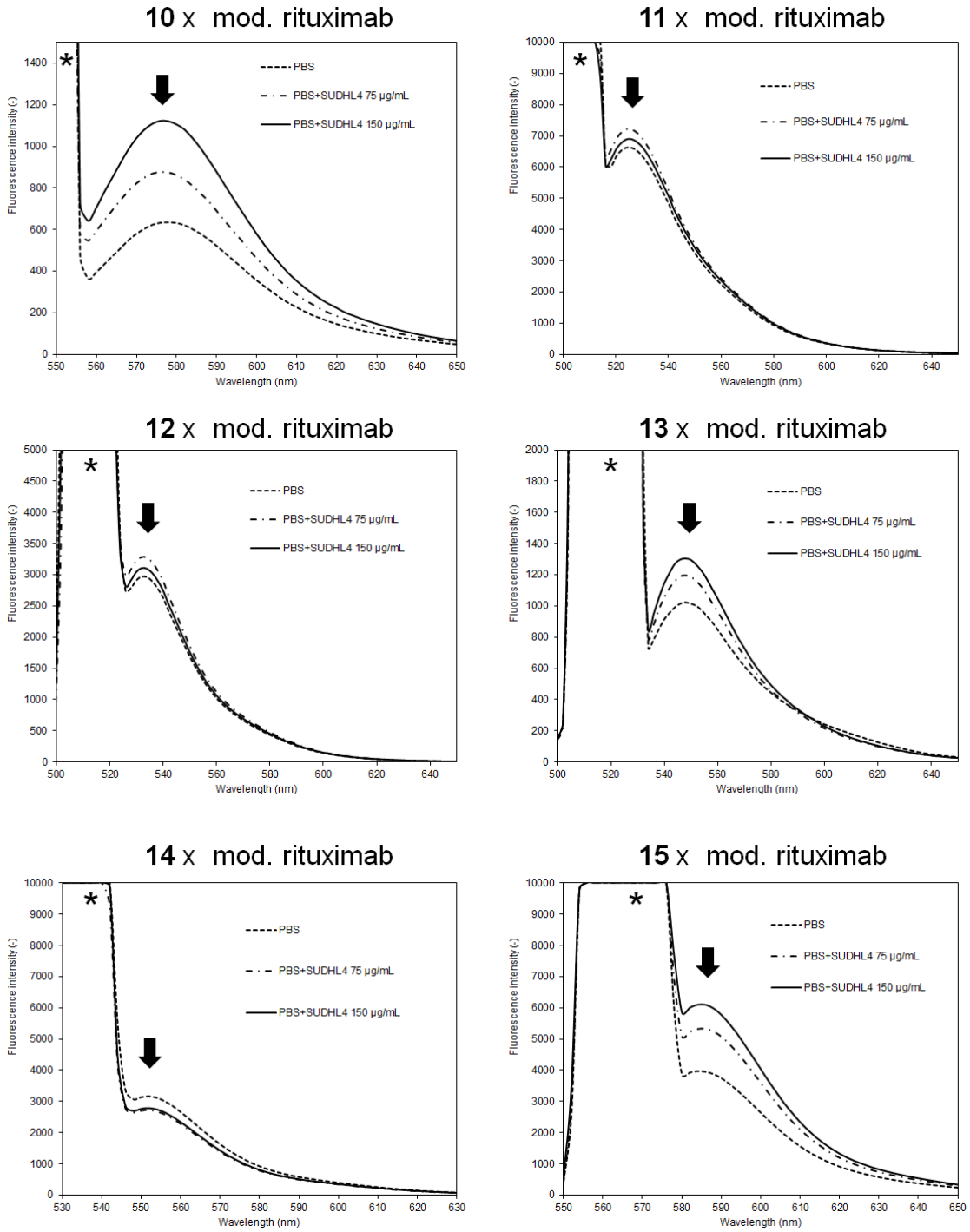

Figures S10. Fluorescence response of modified rituximab to the addition of antigen-expressing cell lysates.

Target emission signals are arrowed. *: Signal derived from the detection of excitation light.

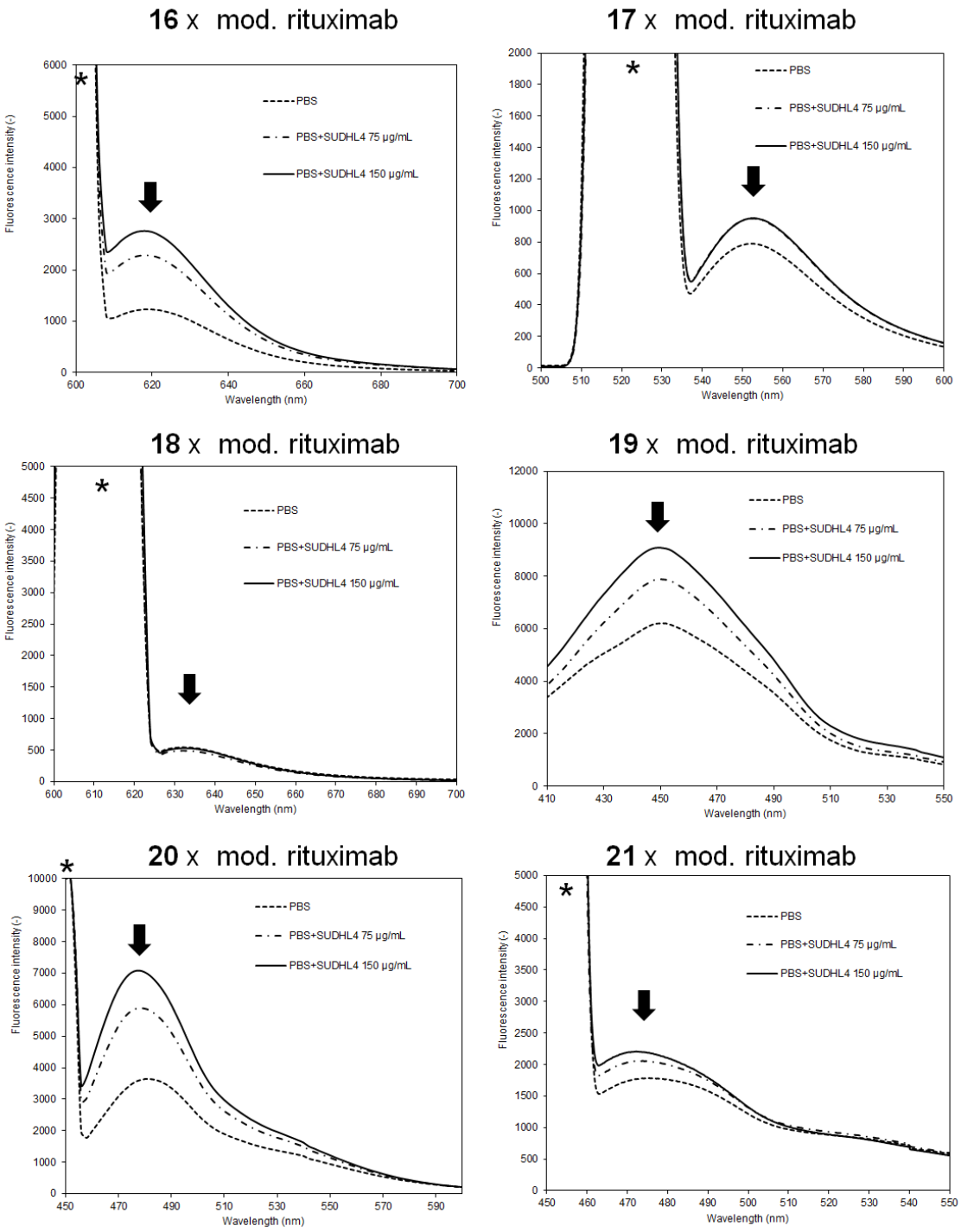

Figure S10 (continued).

Target emission signals are arrowed. *: Signal derived from the detection of excitation light.

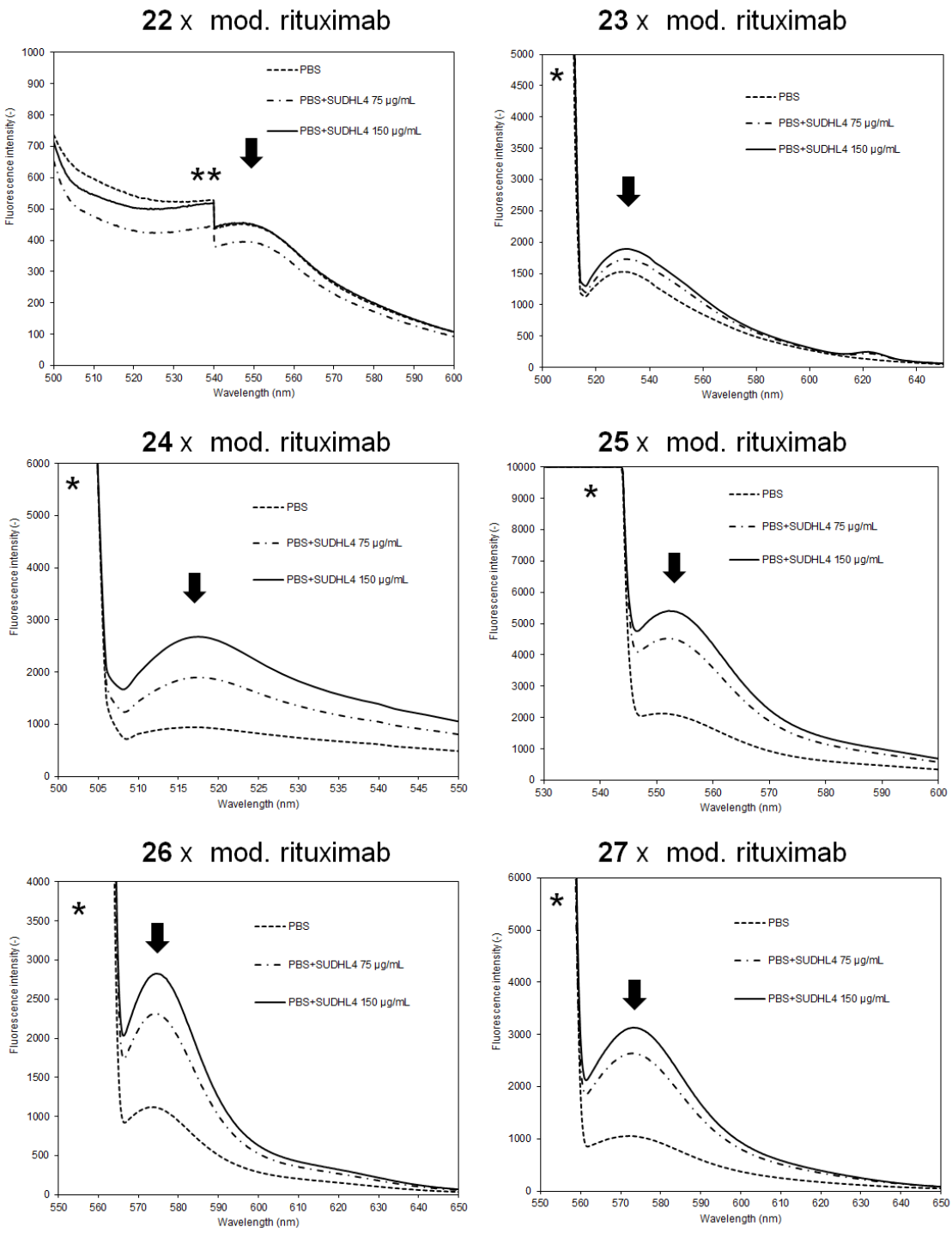

Figure S10 (continued).

Target emission signals are arrowed. *: Signal derived from the detection of excitation light.

**: Mechanical signal change for wavelength filter conversion

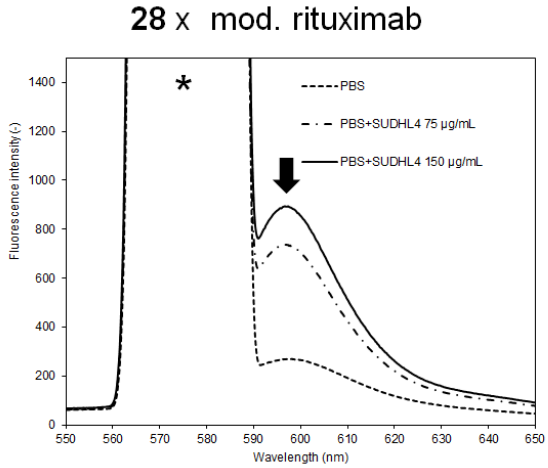

Figure S10 (continued).

Target emission signals are arrowed. *: Signal derived from the detection of excitation light.

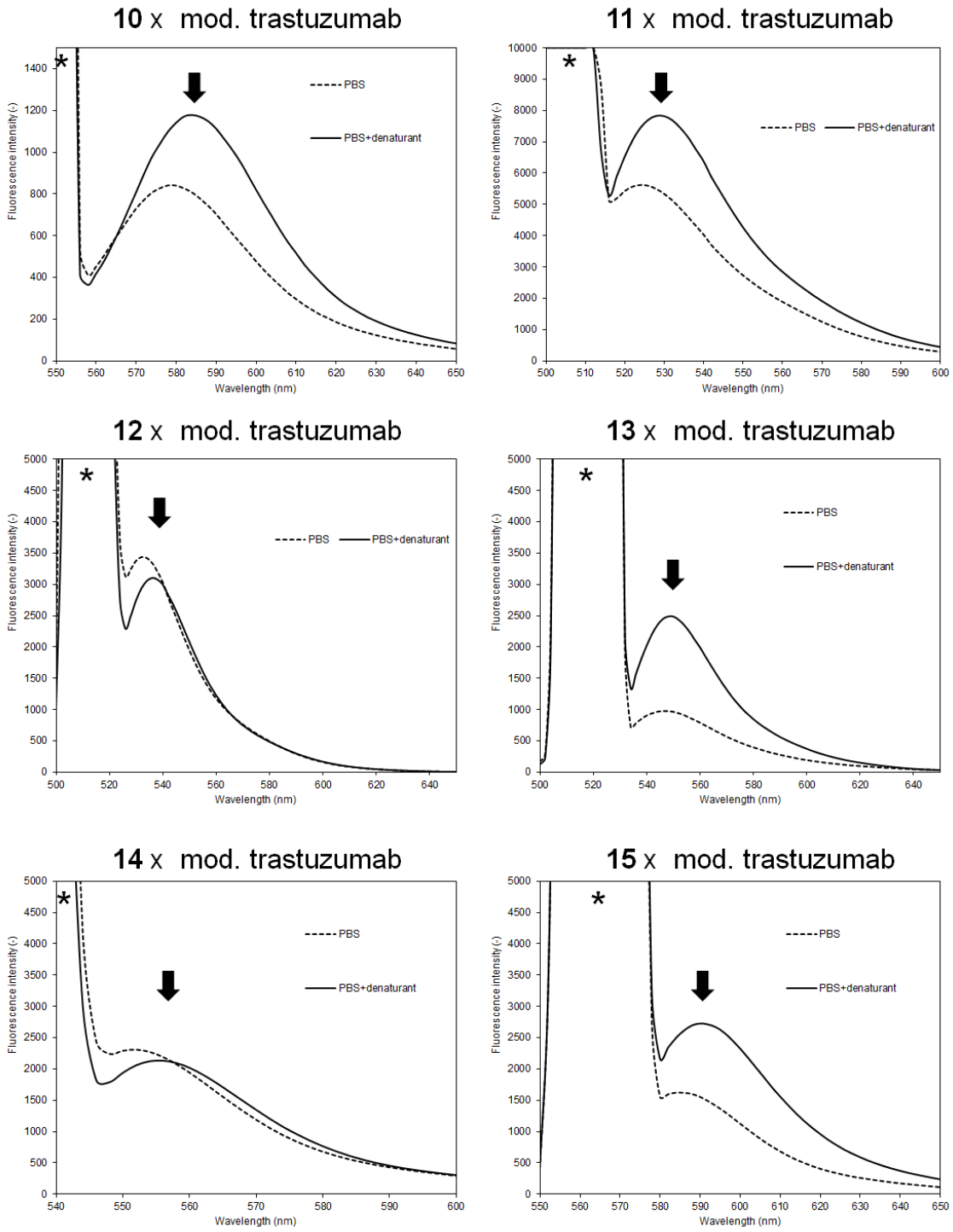

Figures S11. Fluorescent de-quenching of dye-modified trastuzumab in denaturing condition. Target emission signals are arrowed. *: Signal derived from the detection of excitation light.

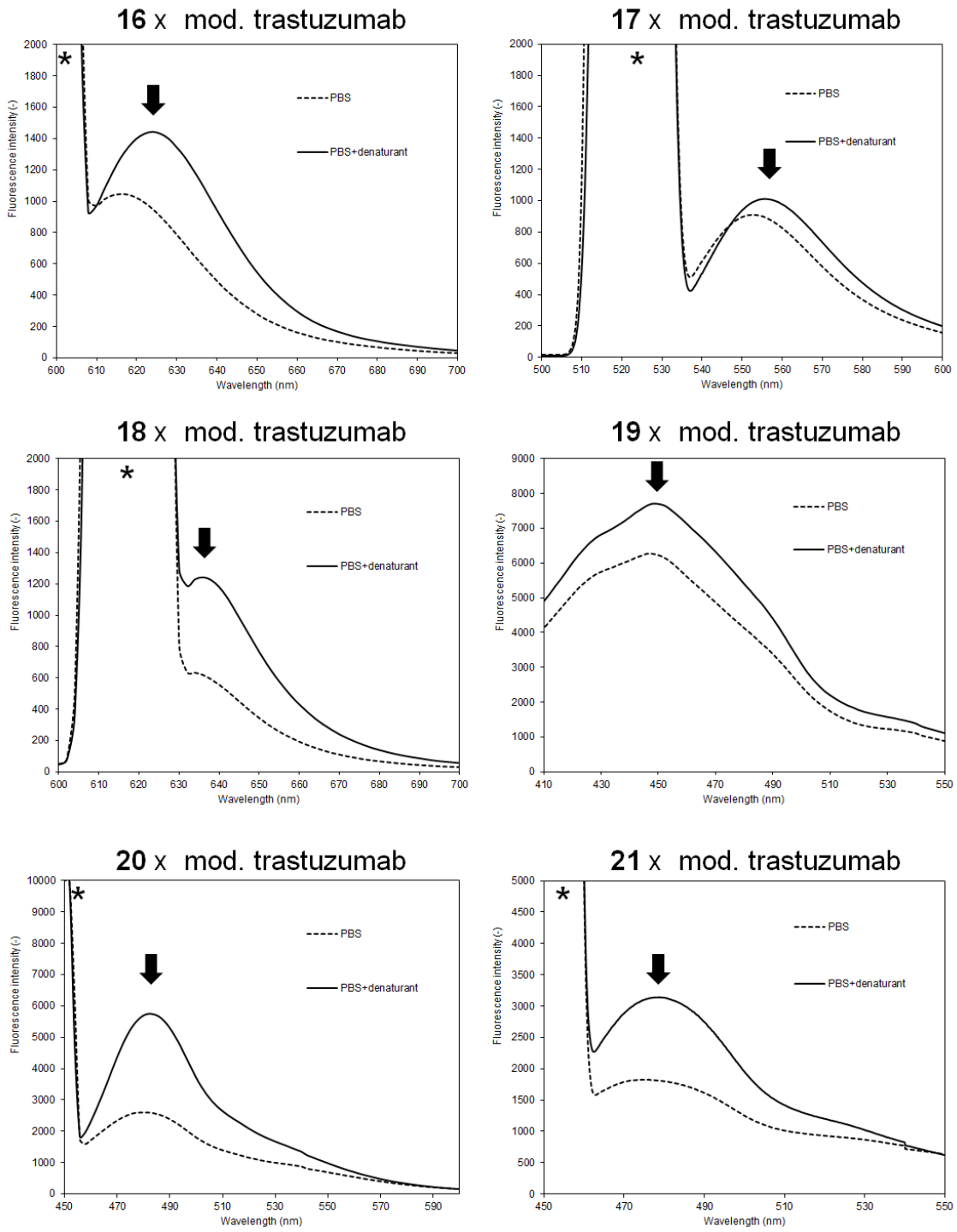

Figure S11 (continued).

Target emission signals are arrowed. *: Signal derived from the detection of excitation light.

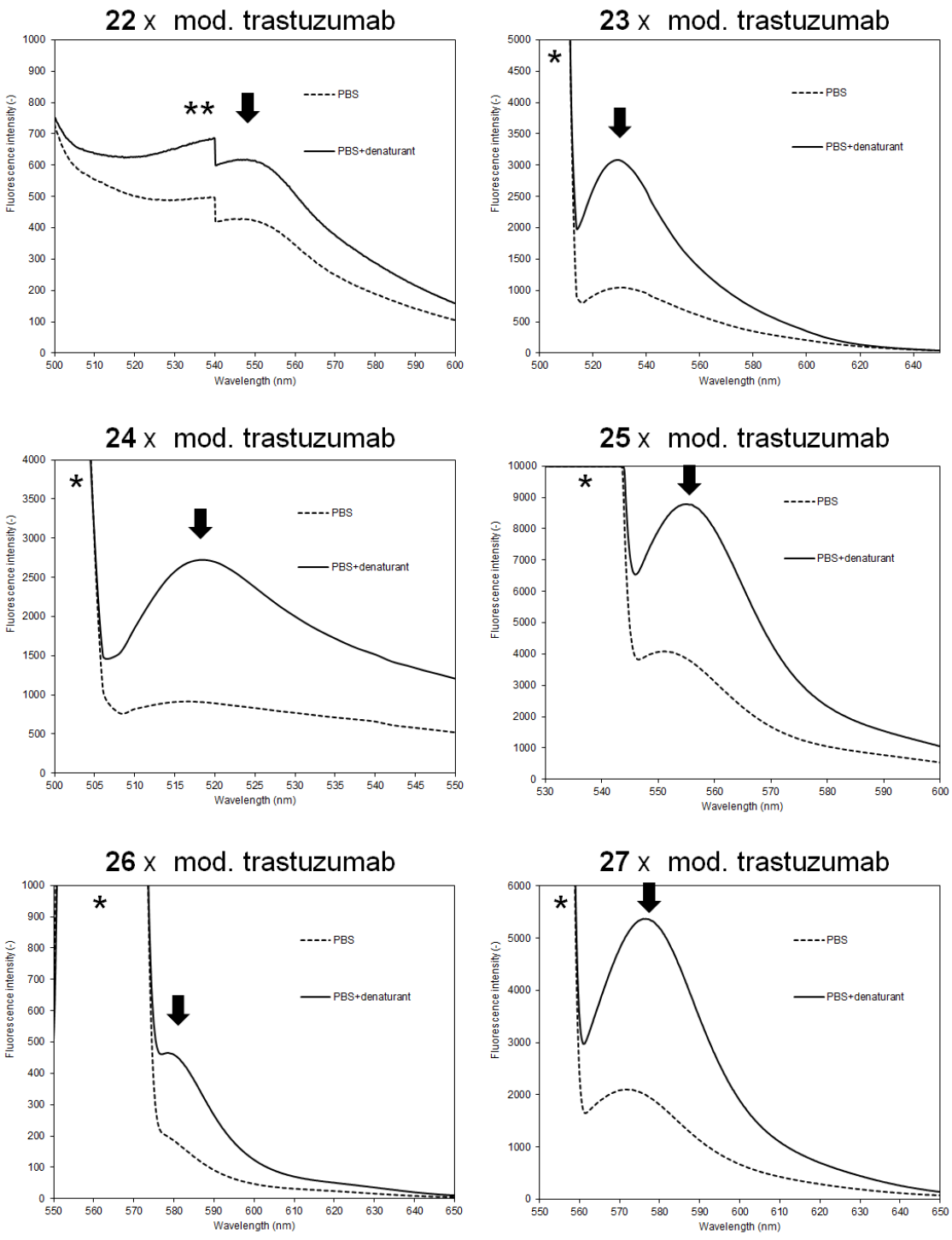

Figure S11 (continued).

Target emission signals are arrowed. *: Signal derived from the detection of excitation light.

**: Mechanical signal change for wavelength filter conversion

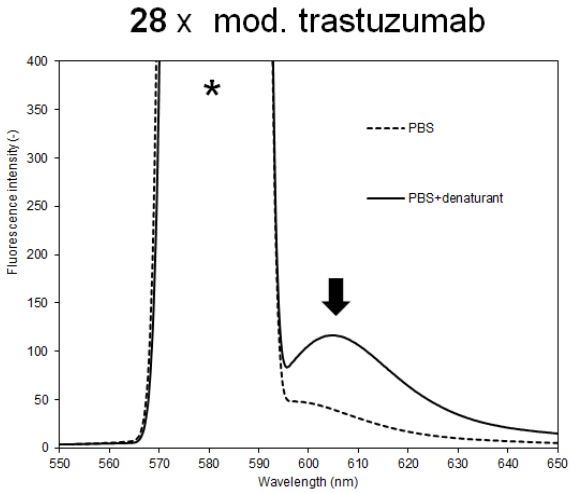

Figure S11 (continued).

Target emission signals are arrowed. *: Signal derived from the detection of excitation light.

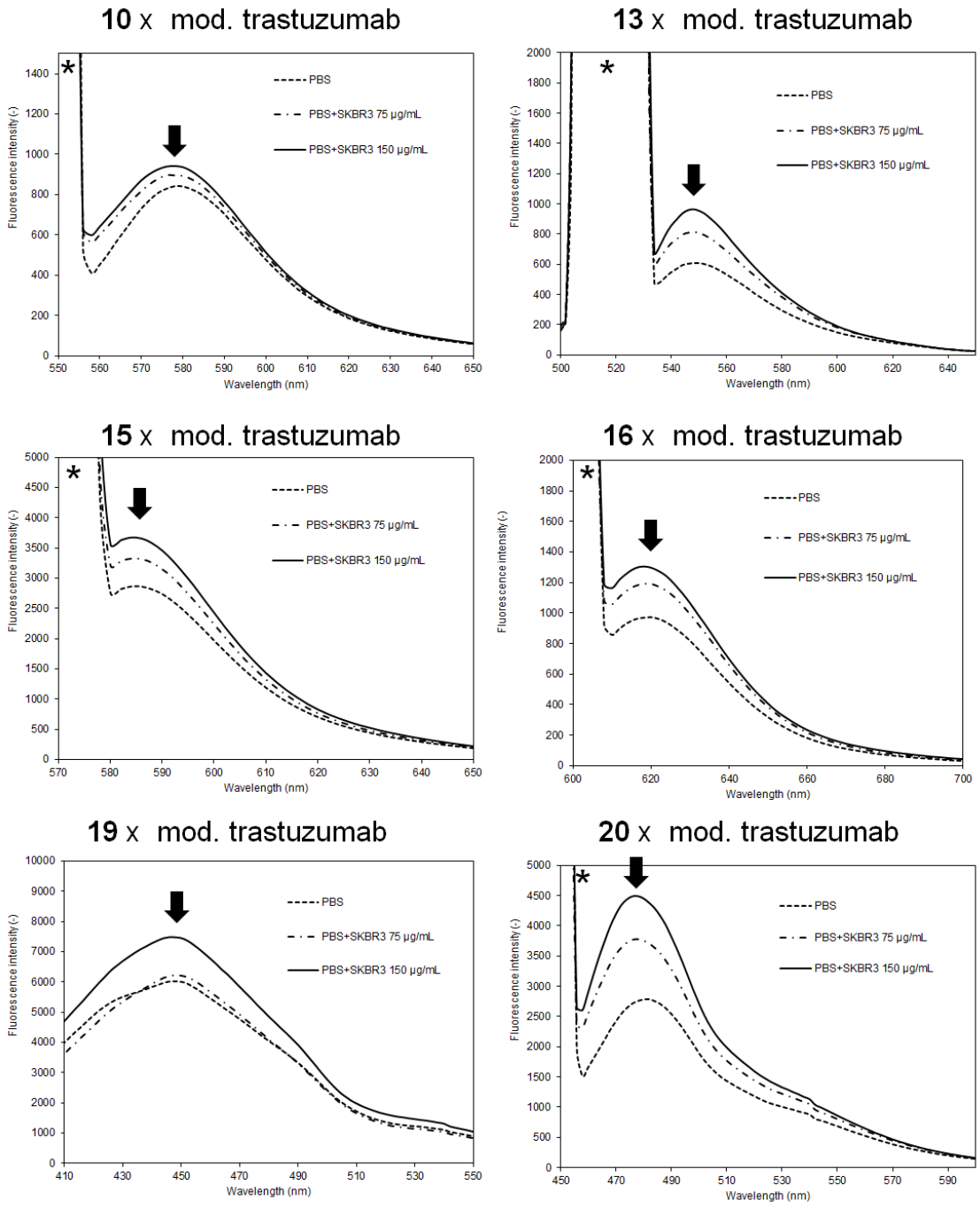

Figures S12. Fluorescence response of modified trastuzumab to the addition of antigen-expressing cell lysates.

Target emission signals are arrowed. *: Signal derived from the detection of excitation light.

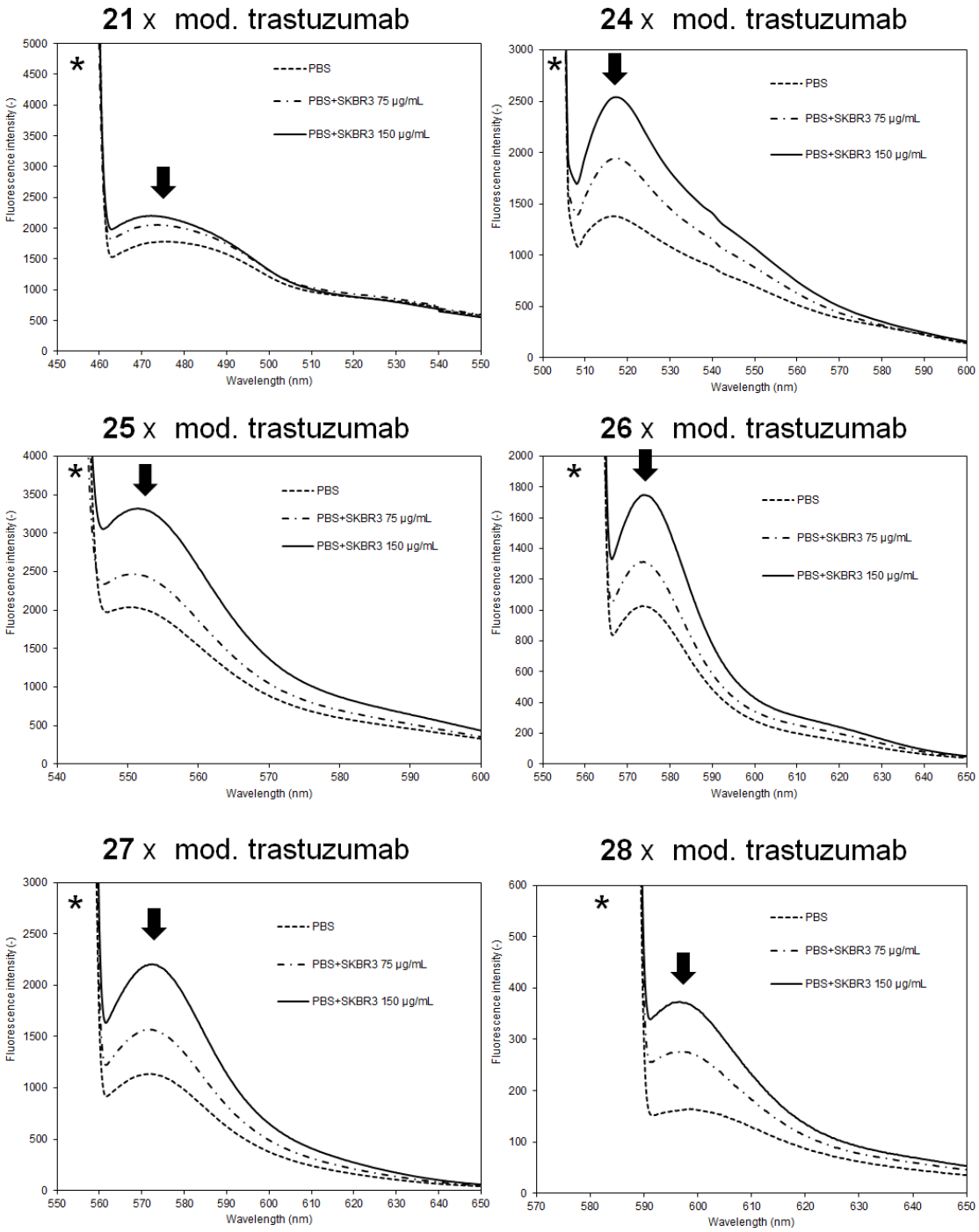

Figure S12 (continued).

Target emission signals are arrowed. *: Signal derived from the detection of excitation light.

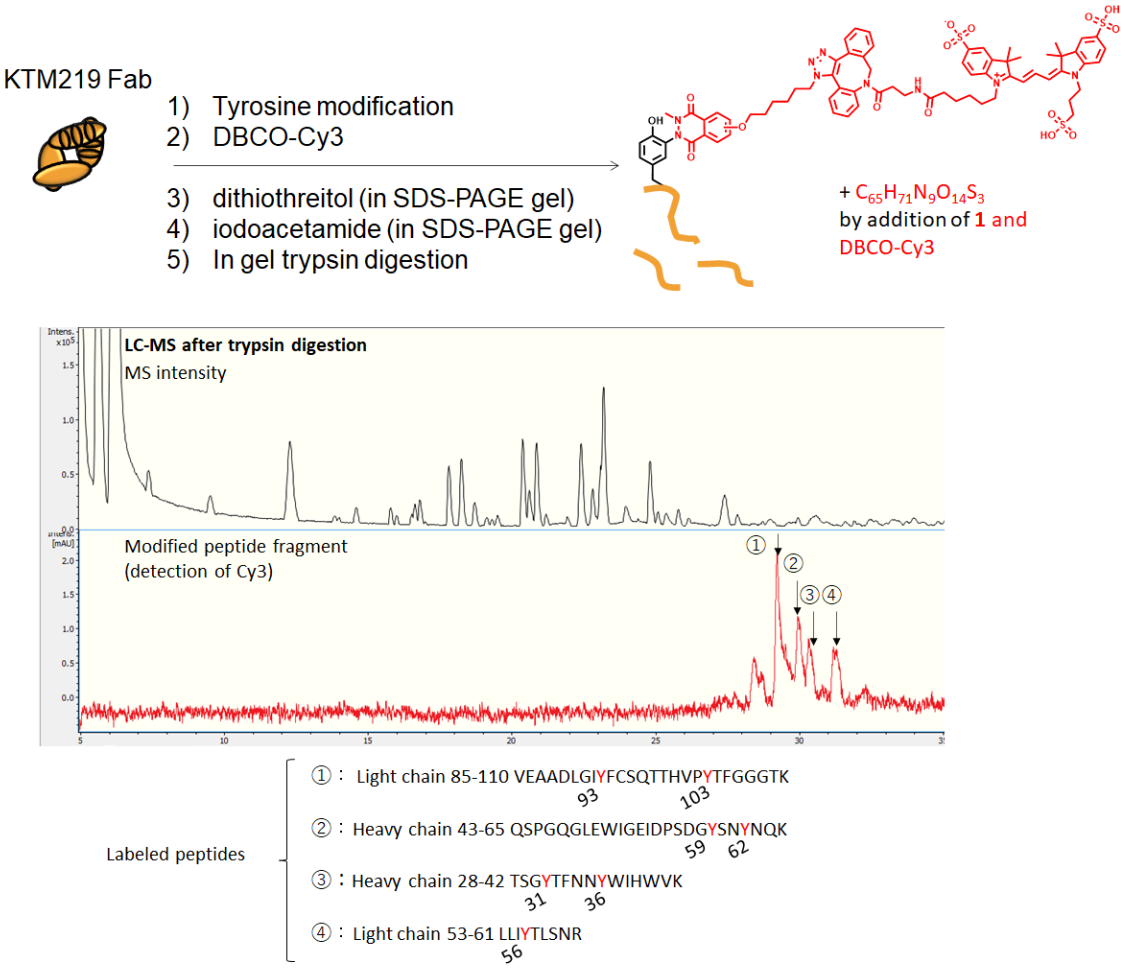

Figures S13. CDR-selective tyrosine modification of KTM219 Fab. LC-MS analysis of peptide fragments obtained by trypsin digestion of modified KTM219 Fab. The peaks were assigned to the peptide containing modified tyrosine in CDR (See Figure S14–17 for MS data).

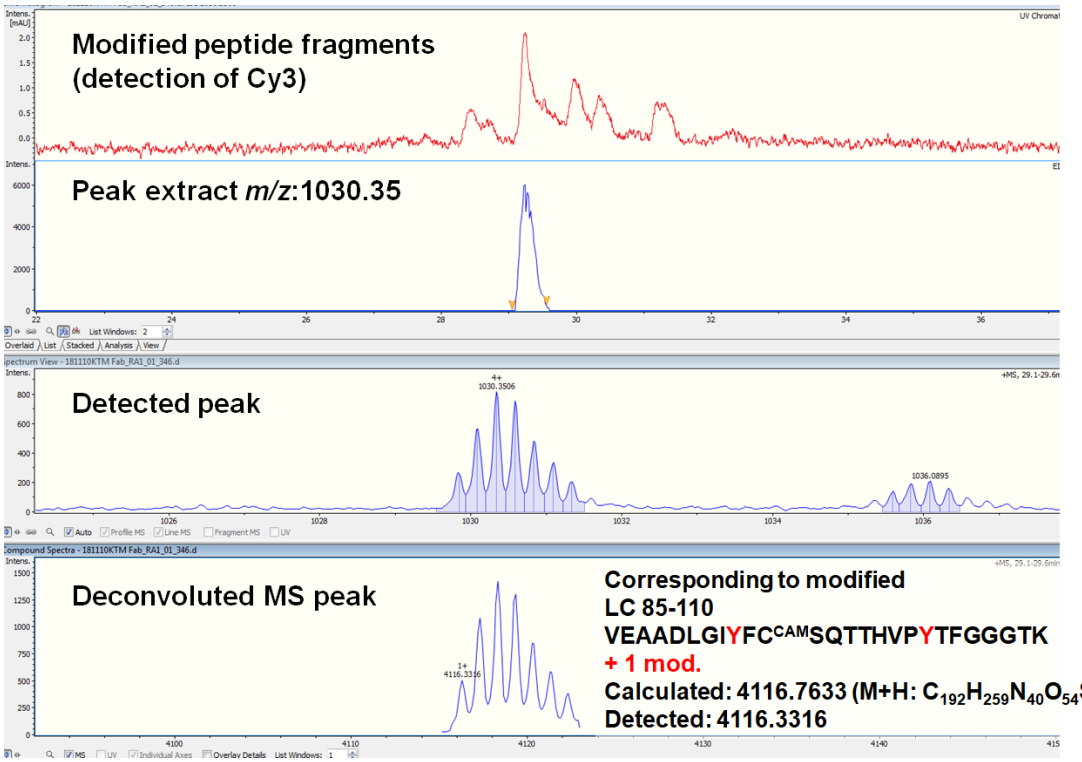

Figures S14. Detected MS peak in LC-MS analysis (retention time: 29.1–29.6 min) shown in Figure S13.

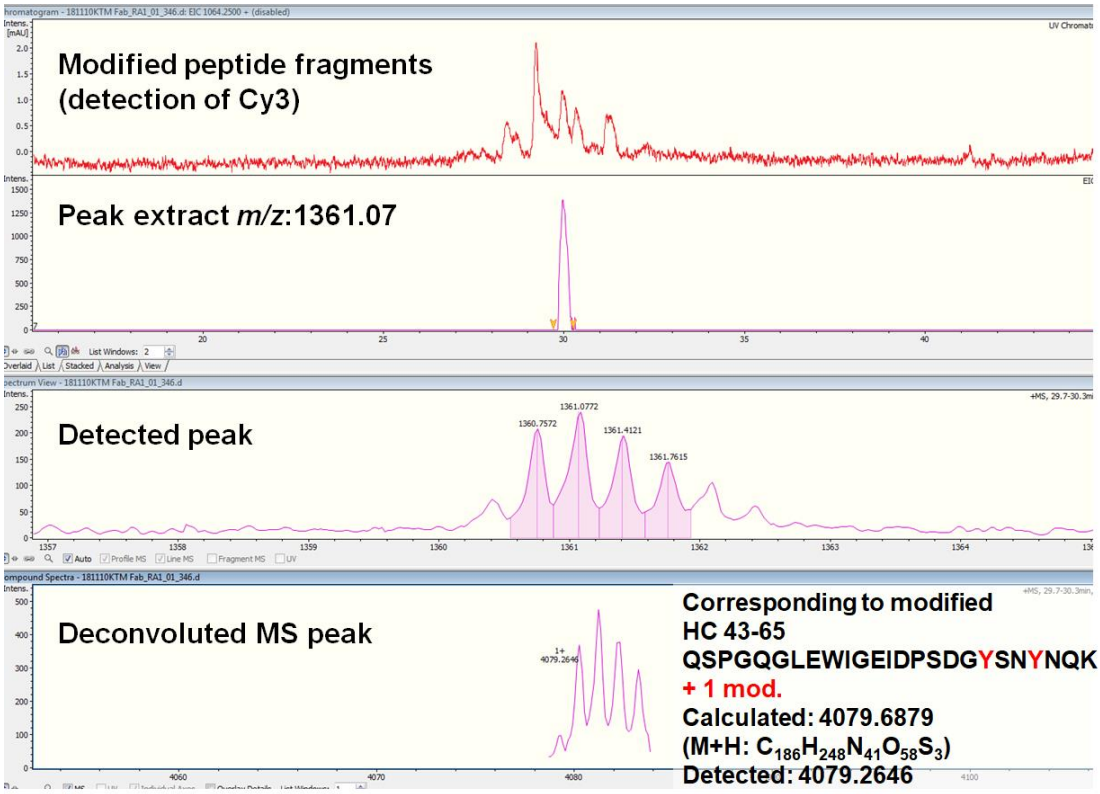

Figures S15. Detected MS peak in LC-MS analysis (retention time: 29.8–30.2 min) shown in Figure S13.

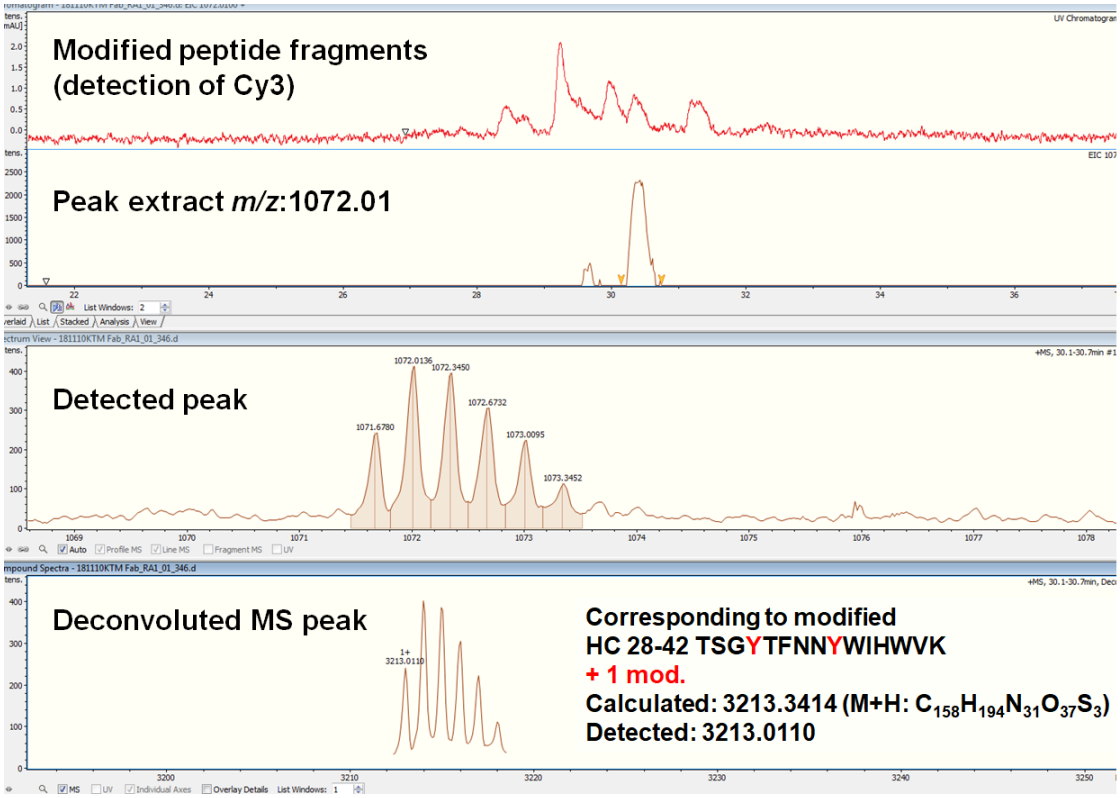

Figures S16. Detected MS peak in LC-MS analysis (retention time: 30.3–30.5 min) shown in Figure S13.

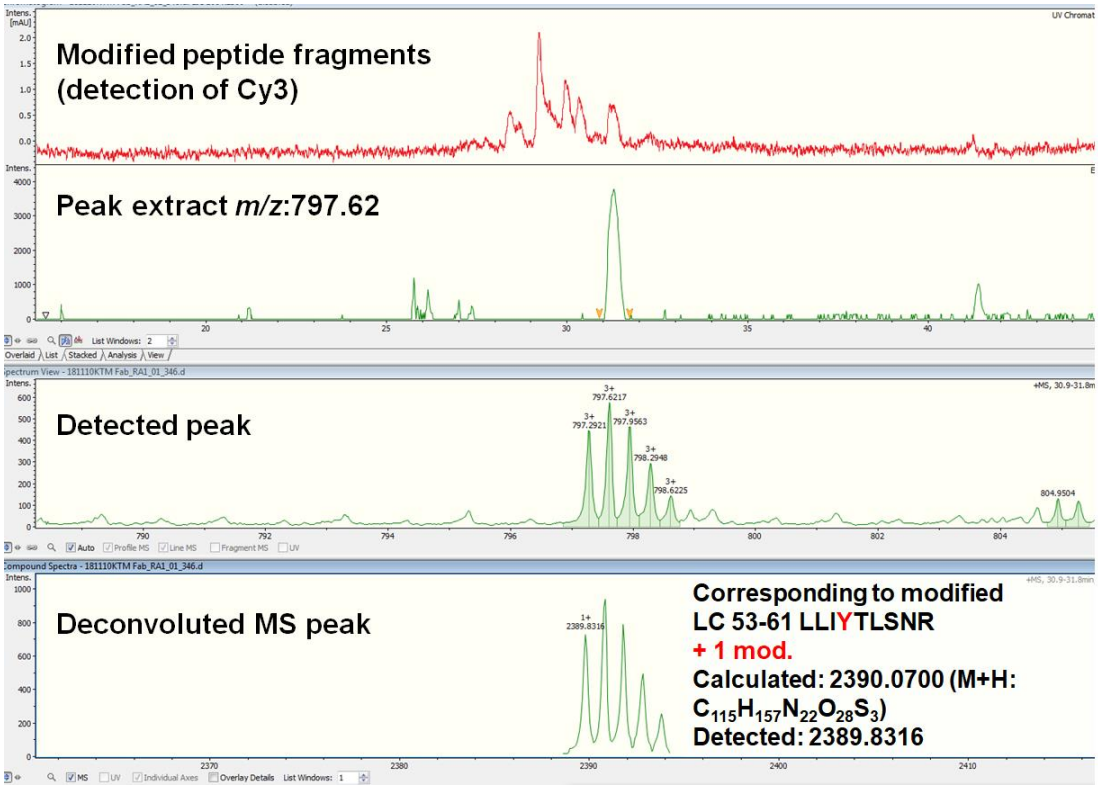

Figures S17. Detected MS peak in LC-MS analysis (retention time: 31.1–31.5 min) shown in Figure S13.

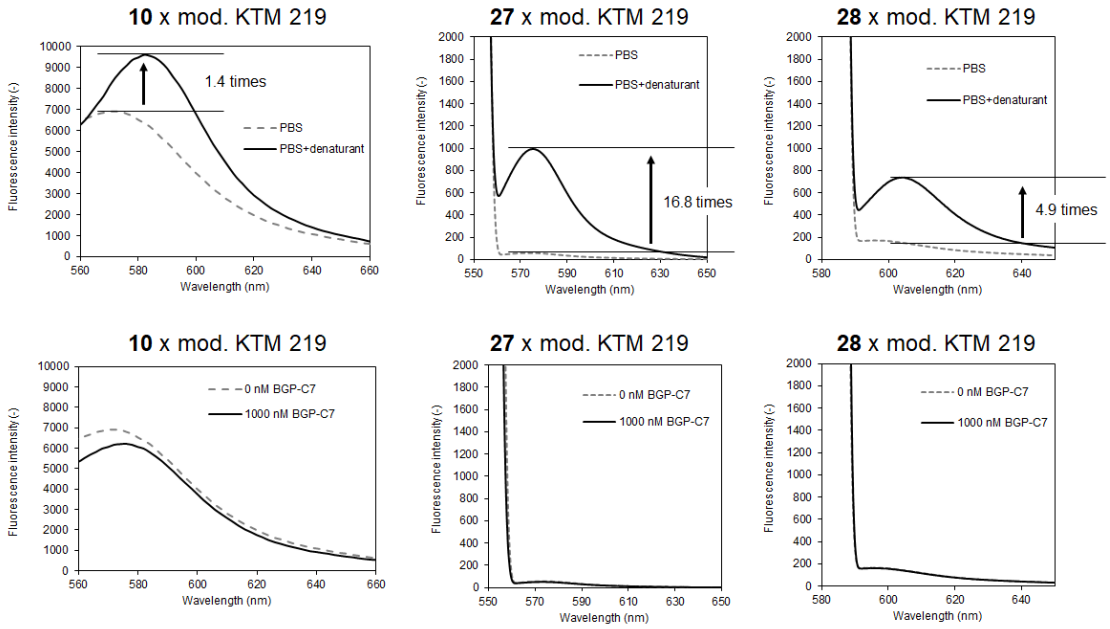

Figures S18. Fluorescence response of modified KTM219 Fab to the denaturing condition (upper) and the addition of antigen (BGP-C7 peptide) (lower).

2. Experimental section

General.

LC-ESI-TOF MS spectra were measured with Bruker micrOTOF II. MALDI-TOF MS spectra were measured using a Bruker Daltonics UltrafleXtreme. The fluorescence spectra were measured with JASCO FP-8300. Most commercially supplied chemicals were used without further purification. All chemicals and purified proteins for biological experiments were obtained from commercial sources and used without further purification. Compounds **1**,[2] **2**,[3] **3**–**4**,[4] **6**,[5] **7**,[5] and **8**[2] were synthesized according to previously reported procedure. Compound **2** was purchased from Sigma Aldrich. Compounds **11**–**16**, **18**–**20**, and **23** were purchased from ATTO TEC. Compounds **17**, **21**, **22**, and **24** were purchased from Thermo Fisher Science. Compounds **25**–**28** were purchased from Lumiprobe.

Antibody modification. (first step) A solution of modification reagent (final conc. 300 μM) was added to a solution of antibody (final conc. 5 μM in 50 mM tris buffered saline (pH7.4) (TBS)). HRP (final conc. 45 nM in 50 mM tris buffer (pH7.4)) and H_2O_2 (final conc. 25 μM in TBS) were added to the mixture, and mixed, then incubated at room temperature for 1 hr. After 1 hr, excess modification reagents were removed using Sephadex G-25 gel (GE Healthcare) filtration columns (2000×g, 4 min). **(second step)** A solution of DBCO-dye (final conc. 10-25 μM) was added to the solution, then incubated at 37 °C for 30 min. After 30 min, excess DBCO-dye were removed using Sephadex G-25 gel (GE Healthcare) filtration columns (2000×g, 4 min). Sephadex G-25 gel filtration removes antibodies aggregated by oxidative damage. The SDS-PAGE was performed using the same amount of protein in each well.

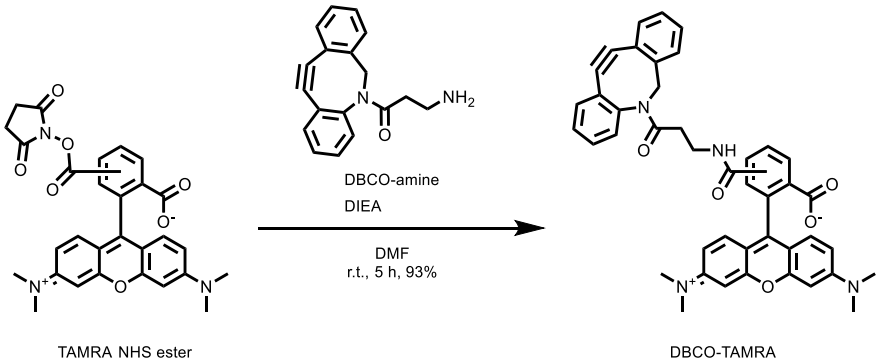

Synthesis of compound 10. To a solution of DBCO-amine solution (100 mM in DMF, 36 μL, 3.6 μmol) and DIEA (100 mM in DMF, 48 μL, 4.8 μmol) in 388 μL of DMF was added 5(6)-TAMRA NHS ester (100 mM, 28 μL in DMF, 2.8 μmol) at room temperature. After stirring at room temperature

for 5 h, the mixture was concentrated in *vacuo*. The residue was purified by PTLC with CH_2Cl_2 : MeOH = 85 : 15 to give 5(6)-DBCO-TAMRA (26 mM in MeOH, 100 µL, 2.6 µmol). The yield was calculated by measuring the absorption spectrum at 535 nm with a microplate reader (TECAN, Infinite F200). The identification and purity of DBCO-TAMRA was confirmed by LC-ESI-TOF MS analysis.

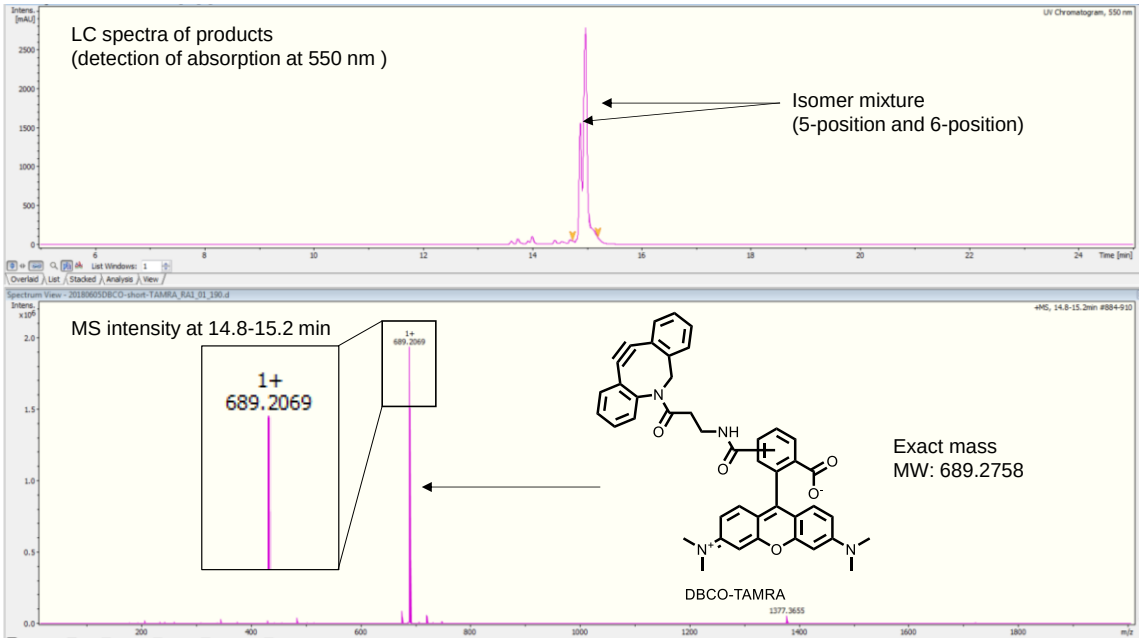

Preparation of DBCO-dye. To a solution of DBCO-amine solution (1 mM in DMF, 2 µL) and DIEA (1 mM in DMF, 2 µL) in 5 µL of DMF was added NHS-dye (1 mM, 1 µL in DMF, Figure 4-18) at room temperature. After stirring at room temperature for 1 h in dark, the mixture was applied to second step of antibody modification without purification.

Fluorescence measurement of Q-body under denaturation condition. Modified antibodies in 1×PBS (or 1×PBS + denaturant (7 M guanidinium hydrochloride and 100 mM dithiotreitol)) was added into polystyrene 10 mm cuvette, then measure fluorescence. The fluorescence emission spectra were obtained at 25 °C.

Fluorescence measurement of Q-body for antigen response evaluation. Labeled antibodies in 1×PBS (or 1×PBS + antigen solution) was added into polystyrene 10 mm cuvette, then was incubated at 25 °C for 2 min prior to the spectral measurements. The fluorescence emission spectra were obtained at 25 °C.

Protein MS of modified antibodies. Modified antibodies (5 μM in 50 mM Tris pH 7.4) was treated with TCEP (final concentration 80 μM), and incubated at room temperature for 1 hr. The reaction mixture was de-salted using ZipTip C4 (Merck) and applied to MALDI-TOF analysis (Bruker, UltrafleXtreme) using sinapinic acid as a matrix.

3. Reference

1 S. Sato, M. Matsumura, T. Kadonosono, S. Abe, T. Ueno, H. Ueda and H. Nakamura, *Bioconjug. Chem.*, 2020, **31**, 1417–1424.

2 S. Sato, K. Nakamura and H. Nakamura, *ACS Chem. Biol.*, 2015, **10**, 2633–2640.

3 S. Sato, K. Nakamura and H. Nakamura, *ChemBioChem*, 2017, **18**, 475–478.

4 S. Sato, M. Yoshida, K. Hatano, M. Matsumura and H. Nakamura, *Bioorganic Med. Chem.*, 2019, **27**, 1110–1118.

5 S. Sato, K. Hatano, M. Tsushima and H. Nakamura, *Chem. Commun.*, 2018, **54**, 5871–5874.